Available online at www.sciencedirect.com
ScienceDirect
Journal of Solid State Chemistry 180 (2007) 3101–3105
JOURNAL OF SOLID STATE CHEMISTRY
www.elsevier.com/locate/jssc

Sonochemical synthesis and luminescence properties of single-crystalline $BaF_2:Eu^{3+}$ nanospheres

Ling Zhu[a,b], Jian Meng[a], Xueqiang Cao[a,*]

[a]*Key Laboratory of Rare Earth Chemistry & Physics, Changchun Institute of Applied Chemistry, Chinese Academy of Sciences, Changchun 130022, Jilin, China*
[b]*Graduate School of the Chinese Academy of Sciences, Beijing 100049, China*

Received 2 June 2007; received in revised form 18 August 2007; accepted 7 September 2007
Available online 14 September 2007

Abstract

BaF_2 nanocrystals doped with 5.0 mol% Eu^{3+} has been successfully synthesized via a facile, quick and efficient ultrasonic solution route employing the reactions between $Ba(NO_3)_2$, $Eu(NO_3)_3$ and KBF_4 under ambient conditions. The product was characterized via X-ray powder diffraction (XRD), scanning electron micrographs (SEM), transmission electron microscopy (TEM), high-resolution transmission electron micrographs (HRTEM), selected area electron diffraction (SAED) and photoluminescence (PL) spectra. The ultrasonic irradiation has a strong effect on the morphology of the $BaF_2:Eu^{3+}$ particles. The caddice-sphere-like particles with an average diameter of 250 nm could be obtained with ultrasonic irradiation, whereas only olive-like particles were produced without ultrasonic irradiation. The results of XRD indicate that the obtained $BaF_2:Eu^{3+}$ nanospheres crystallized well with a cubic structure. The PL spectrum shows that the $BaF_2:Eu^{3+}$ nanospheres has the characteristic emission of Eu^{3+} $^5D_0$–^7F_J ($J = 1$–4) transitions, with the magnetic dipole $^5D_0$–$^7F_1$ allowed transition (590 nm) being the most prominent emission line.

Keywords: Ultrasonic irradiation; $BaF_2:Eu^{3+}$; Solution route; Luminescence

1. Introduction

It is well known that the size and shape of inorganic crystals have great influence on their chemical and physical properties. For instance, the optical properties of luminescent nanomaterials are enormously affected by their shapes and sizes [1–3]. Therefore, the synthesis of nanoparticles with well-controlled shapes, sizes, and structures is both scientifically and technically important. So far, much effort has been employed to fabricate nanomaterials with unique shapes, such as ZnO doughnuts [4], Cu_2O flowers [5], NiS with urchin-like nanostructures [6], dendritic micro-pines of magnetic a-Fe_2O_3 [7], ZnO cup [8], etc. Thus, further explorations of novel morphology of inorganic materials by convenient synthesis methods, is of great importance. Owing to the great chemical flexibility and synthetic tenability in the solution-phase synthesis, the solution-based approaches provide a simple process toward various nanomaterials. Because of significant advantages, such as low temperature, cost-effective and less-complicated techniques, sonochemical method has emerged as a powerful tool for the fabrication of inorganic nanomaterials with novel morphologies [9–11]. The chemical effects of ultrasound arise from acoustic cavitation including the formation, growth, pulsation and collapse of tiny bubbles in liquids. When solution is exposed to strong ultrasound irradiation, bubbles in the solution are implosively collapsed by acoustic fields, producing transient micro "hot spots", which can reach temperatures as high as 5000 K and pressures over 1800 atm, and the cooling rate can be in excess of 10^{10} K s^{-1}[12,13]. These extreme transient high pressures and temperatures provide a unique environment for the growth of materials with novel structures and can promise a very short reaction time [14].

Up to now, most reports concerning luminescent materials have concentrated on oxygen-based systems, such as oxides and inorganic salts [15–18]. However, the

*Corresponding author. Fax: +86 431 85262285.
E-mail address: xcao@ciac.jl.cn (X. Cao).

0022-4596/$ - see front matter © 2007 Elsevier Inc. All rights reserved.
doi:10.1016/j.jssc.2007.09.010

conventional oxygen-based systems often have large phonon energy as a result of the stretching vibrations of the host molecules [19]. In comparison, fluorides have an advantage as a fluorescent host matrix owing to their low vibrational energies, and the subsequent minimization of quenching of the excited state of the rare earth ions [20–22]. Trivalent rare earth ions doped MF_2 (M = Ba, Sr, Ca) crystals, characterized by low phonon energy and large transfer coefficient between rare earth ions, have been of great interest owing to their potential applications in microelectronic and optoelectronic devices, such as wide-gap insulating overlayers, gate dielectrics, insulators, and buffer layers in semiconductor-on-insulator structures and more advanced 3D devices [23–25]. BaF_2 activated with rare earth ions have also been reported to display unique luminescence properties and can be used as scintillators [26]. The investigation on the preparation and properties of BaF_2 has attracted a great deal of attention, and a variety of methods have been employed to fabricate this material, including the flame spray method [27], the microemulsion process [28], the reverse microemulsions [29], and the hydrothermal method [30,31]. Recently, BaF_2 nanowires and nanocubes with arching sheet-like dendrites have been prepared in quaternary microemulsions and reverse micelles, respectively [32,33]. However, to the best of our knowledge, the synthesis of single-crystalline BaF_2:Eu^{3+} with the caddice-sphere-like nanostructure has not yet been reported. Herein, we report a facile and fast sonochemical method to synthesize the single crystal of BaF_2:Eu^{3+} caddice-spheres without any template or organic additive, and further investigate its microstructure and luminescent properties.

2. Experimental section

2.1. Synthesis

All the reagents used in this work were of analytical grade, including $Ba(NO_3)_2$ and KBF_4 (Beijin Chemical Reagent), Eu_2O_3 (Shanghai Chemical Reagent). In a typical synthesis, appropriate amounts of Eu_2O_3 was first dissolved in 10% nitric acid, and then mixed with another solution containing 1.00 g $Ba(NO_3)_2$ (Ba:Eu = 95:5, in molar ratio) and KBF_4 (100% excess). The resulting solution was sonicated at ambient temperature for 3 h by a high-intensity ultrasonic probe (JCS-206 Jining Co. China, Ti-horn, 23 kHz). A white precipitate was centrifuged, washed with distilled water and absolute ethanol in sequence. The final product was dried under vacuum at 60 °C for 12 h. For comparison, a sample of BaF_2:Eu^{3+} was also synthesized via vigorous stirring under the same conditions but without ultrasonic irradiation.

2.2. Characterization

The X-ray powder diffraction (XRD) pattern was performed on a Rigaku D/MAX-2500 diffractometer with Cu $K\alpha$ radiation (λ = 0.15406 nm) and a scanning rate of 5° min^{-1}. Scanning electron micrographs (SEM) images were taken on a XL30 field-emission scanning electron microscope. Transmission electron microscopy (TEM), high-resolution transmission electron micrographs (HRTEM) and selected area electron diffraction (SAED) patterns were recorded on a JEOL-JEM-2010 operating at 200 kV (JEOL, Japan). Sample for TEM was prepared by dropping a diluted suspension of the sample powders onto a standard carbon-coated (20–30 nm) Formvar film on a copper grid (230 mesh). Photoluminescence (PL) spectra were recorded with a Hitachi F-4500 spectrophotometer equipped with a 150 W Xenon lamp as the excitation source. All the measurements were performed at room temperature.

3. Results and discussion

3.1. Structure and morphology control of the nanocrystal

As shown in Fig. 1, the XRD patterns of the two samples prepared with or without ultrasonic irradiation are similar and are consistent with the cubic phase BaF_2 (JCPDS No. 04-0452). The strong and sharp diffraction peaks indicate that the products are well crystallized. Fig. 2a–b show the SEM images of the as-formed BaF_2:Eu^{3+} sample prepared via the sonochemical method. It can be seen that the BaF_2:Eu^{3+} sample is composed of caddice-spheres with average diameter of 250 nm (Fig. 2a). An enlarged SEM image (Fig. 2b) displays that the surface of the caddice-sphere is very scraggy. Fig. 2c is the TEM image of the BaF_2:Eu^{3+} spheres. The SAED image (Fig. 2e) indicates that the as-formed BaF_2:Eu^{3+} caddice-sphere is single crystalline. The clear lattice fringes in the HRTEM image (Fig. 2d) confirm the high crystallinity of the as-prepared BaF_2:Eu^{3+} caddice-spheres. Fig. 3a is the SEM image of sample synthesized via stirring method, indicating the

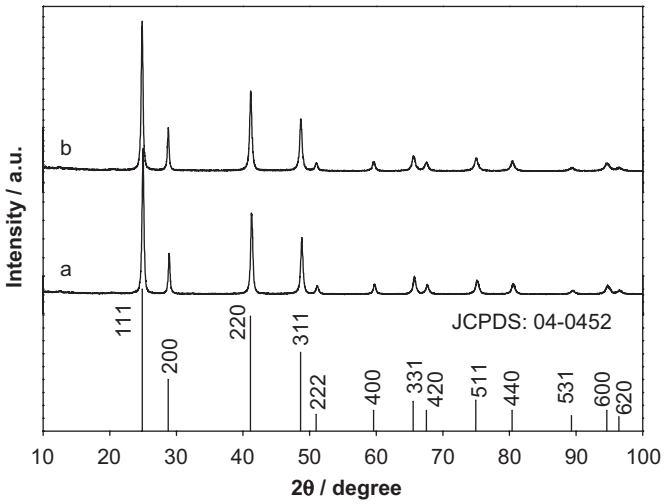

Fig. 1. XRD patterns of BaF_2:Eu^{3+} samples synthesized by (a) ultrasonic irradiation, and (b) stirring.

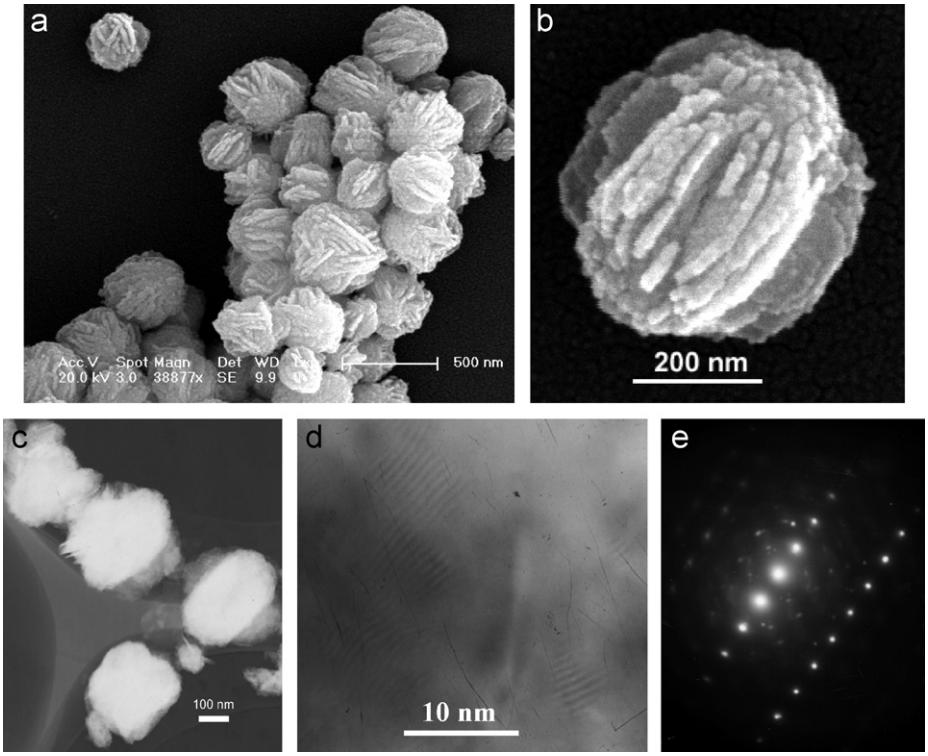

Fig. 2. (a, b) SEM images with different magnification, (c) TEM, (d) HRTEM, and (e) SAED images of the BaF_2:Eu^{3+} nanocrystal via sonochemical method.

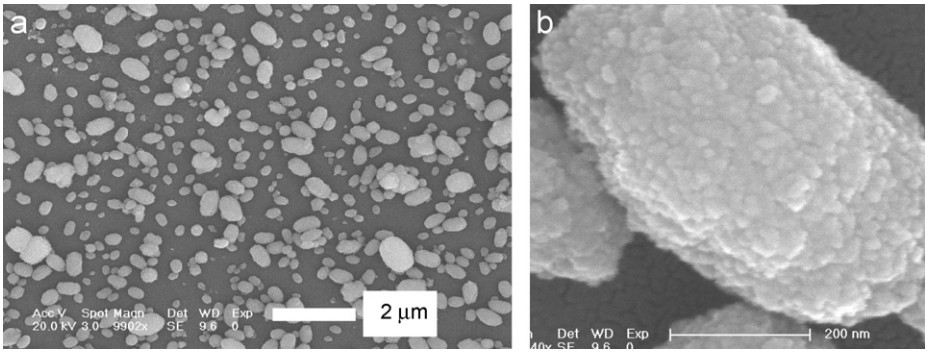

Fig. 3. (a, b) SEM images with different magnification of the as-prepared BaF_2:Eu^{3+} nanocrystal via stirring.

olive-like morphology with a diameter of 200–450 nm and length from 260 to 800 nm. Furthermore, the olive-like particles are composed of nanosized particles with diameter ranging from 30 to 45 nm, as can be clearly observed from the magnified image (Fig. 3b).

Obviously, the ultrasonic irradiation plays an important role and is found to be necessary to the synthesis of BaF_2:Eu^{3+} with the caddice-sphere-like structure in the current case, due to the fact that only olive-like product was obtained in the absence of ultrasonic irradiation (Fig. 3a). The formation of BaF_2:Eu^{3+} with the caddice-sphere morphology may be explained as follows. In aqueous solution KBF_4 was slowly hydrolyzed to produce F^-; these F^- anions react with Ba^{2+}, and Eu^{3+} cations to form BaF_2:Eu^{3+} shown in the following equations [34]:

$$BF_4^- + 3H_2O \overset{)))))))}{\longleftrightarrow} H_3BO_3 + 3HF + F^- \quad (K^\theta = 6.41 \times 10^{-12} \text{ at } 25\,^\circ\text{C}) \tag{1}$$

$$Ba^{2+} + 2F^- \overset{)))))))}{\longrightarrow} BaF_2 \downarrow . \tag{2}$$

The equilibrium-constant of the hydrolysis reaction (Eq. (1)) is very small, which will keep the low concentration of F^- ions in the reaction solution, and consequently lead to the slow crystallization process. However, the employing of the ultrasonic irradiation will accelerate the hydrolysis process, which is presumably helpful to the nucleation and growth of the BaF_2:Eu^{3+} nanocrystals.

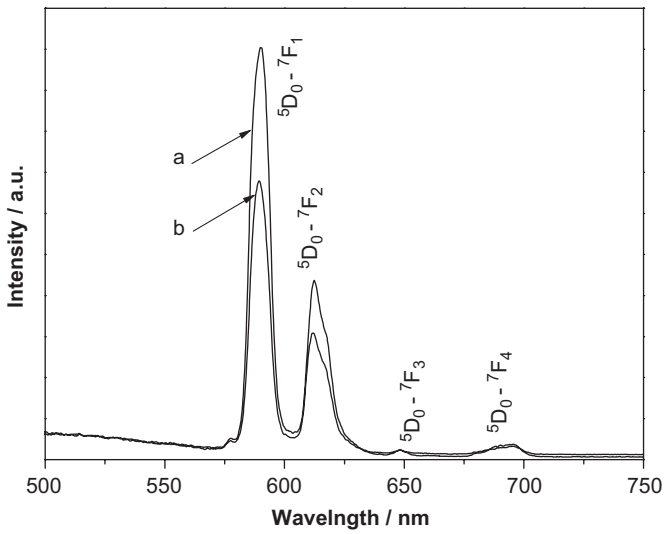

Fig. 4. Emission spectra of BaF_2:Eu^{3+} nanocrystals synthesized by (a) ultrasonic irradiation, and (b) stirring.

Furthermore, the cavitation and shock wave created by the ultrasound can accelerate solid particles to high velocities, leading to the interparticle collision and effective fusion at the point of collision. Such cavitation behavior leads to many unique properties in the irradiated solution and has been used extensively to generate materials with interesting morphologies.

3.2. Optical properties

Fig. 4 presents the room temperature emission spectra of BaF_2:Eu^{3+} products which were obtained in the presence and absence of ultrasound irradiation. Both the samples were measured under the identical conditions with the excitation wavelength of $\lambda_{ex} = 397$ nm. The emission spectra of these two samples show similar patterns (Fig. 4a–b). The characteristic emission peaks of Eu^{3+} within the wavelength range from 550 to 720 nm were observed, corresponding to the transitions from the excited $^5D_0$ level to ^7F_J ($J = 1$–4) levels, with the magnetic dipole $^5D_0$–$^7F_1$ allowed transition (590 nm) being the most prominent emission line [30]. As is well known, the $^5D_0$–$^7F_1$ lines originate from magnetic dipole transition, while the $^5D_0$–$^7F_2$ lines originate from electric dipole transition. In terms of the Judd–Ofelt theory [35,36], the magnetic dipole transition is permitted. The electric dipole transition is allowed only on the condition that the europium ion occupies a site without an inversion center and is sensitive to local symmetry. Therefore, when europium ions occupy inversion center sites, the $^5D_0$–$^7F_1$ transition should be relatively strong, while the $^5D_0$–$^7F_2$ transition should be relatively weak. In the current case, the intensity ratios of $^5D_0$–$^7F_2$ to $^5D_0$–$^7F_1$ in caddice-spheres and olive-like particles were determined to be 0.48 and 0.55, respectively. These results indicate that in the caddice-spheres more Eu^{3+} ions occupy inversion center sites in comparison with the olive-like particles.

Although the PL positions of these two samples are identical, the PL intensity is different with the caddice-spheres is higher (about 32%) than that of the olive-like product under the same measurement conditions. Normally, such differences in the PL spectra can be caused by factors like the extent of crystallinity, morphology, size distribution, homogeneity and dimension of the luminescent material. XRD studies revealed that the caddice-spheres (Fig. 1a) and the olive-like product (Fig. 1b) prepared with or without ultrasonic irradiation are highly crystalline with the same crystal structure and similar crystal intensity. Therefore, the different in the PL intensity may be due to the different morphologies and size distributions of these two samples, which have similarly been observed by other researchers [37–39]. The olive-like crystals may have more defects. Some of these defects act as nonradiative recombination centres and may be responsible for the decrease of the PL intensity of the olive-like product.

4. Conclusion

In summary, the use of ultrasonic irradiation in the synthesis of BaF_2:Eu^{3+} particles has a remarkable effect on the morphology of the particles produced. BaF_2:Eu^{3+} caddice-spheres were formed in the presence of ultrasonic irradiation, whereas only olive-like particles were obtained in the absence of ultrasonic irradiation. This simple and unique synthetic method without any template or surfactant, which avoids the subsequent complicated workup procedures for the removal of the template or surfactant, has a potential advantage for synthesis of material with novel morphology. The PL result reveals that these two BaF_2:Eu^{3+} samples with different morphologies show the similar characteristic emission of Eu^{3+} $^5D_0$–^7F_J ($J = 1$–4) transitions, but the emission intensity of the caddice-spheres was higher than that of the olive-like product under the same measurement conditions.

Acknowledgments

We gratefully acknowledge the financial support from NSFC 20471058. We also appreciate the help from Ms. M.Y. Li and Mr. L.H. Ge in the measurements of SEM and TEM.

References

[1] H.W. Song, J.W. Wang, J. Lumin. 118 (2006) 220.
[2] A.L. Pan, H. Yang, R. Yu, B.S. Zoul, Nanotechnology 17 (2006) 1083.
[3] J. Hu, L. Li, W. Yang, L. Manna, L. Wang, A.P. Alivisatos, Science 292 (2001) 2060.
[4] T. Ghoshal, S. Kar, S. Chaudhuri, Cryst. Growth Des. 7 (2007) 136.
[5] Y.S. Luo, S.Q. Li, Q.F. Ren, J.P. Liu, L.L. Xing, Y. Wang, Y. Yu, Z.J. Jia, J.L. Li, Cryst. Growth Des. 7 (2007) 87.
[6] W.Q. Zhang, L.Q. Xu, K.B. Tang, F.Q. Li, Y.T. Qian, Eur. J. Inorg. Chem. (2005) 653.

[7] M.H. Cao, T.F. Liu, S. Gao, G.B. Sun, X.L. Wu, C.W. Hu, Z.L. Wang, Angew. Chem. Int. Ed. 44 (2005) 4197.
[8] Y.S. Fu, X.W. Du, J. Sun, Y.F. Song, J. Liu, J. Phys. Chem. C 111 (2007) 3863.
[9] J. Geng, Y.N. Lv, D.J. Lu, J.J. Zhu, Nanotechnology 17 (2006) 2614.
[10] X.L. Wu, M.H. Cao, C.W. Hu, X.Y. He, Cryst. Growth Des. 6 (2006) 26.
[11] G.T. Zhou, J.C. Yu, X.C. Wang, L.Z. Zhang, New J. Chem. 28 (2004) 1027.
[12] S.J. Doktycz, K.S. Suslick, Science 247 (1990) 1067.
[13] E.B. Flint, K.S. Suslick, Science 253 (1991) 1397.
[14] V.G. Pol, O. Palchik, A. Gedanken, I. Felner, J. Phys. Chem. B 106 (2002) 9737.
[15] P.A. Tanner, K.L. Wong, J. Phys. Chem. B 108 (2004) 136.
[16] S. Lemanceau, G. Bertrand-Chadeyron, R. Mahiou, M. El-Ghozzi, J.C. Cousseins, P. Conflant, R.N. Vannier, J. Solid State Chem. 148 (1999) 229.
[17] A. Huignard, T. Gacoin, J.P. Boilot, Chem. Mater. 12 (2000) 1090.
[18] L.D. Sun, C.S. Liao, C.H. Yan, J. Solid State Chem. 171 (2003) 304.
[19] Y.W. Zhang, X. Sun, R. Si, L.P. You, C.H. Yan, J. Am. Chem. Soc. 127 (2005) 3260.
[20] I.A. Cárcer, P. Herrero, A.R. Landa-Cánovas, B. Sobolev, Appl. Phys. Lett. 87 (2005) 053105.
[21] S. Heer, K. Kömpe, H.U. Güdel, M. Haase, Adv. Mater. 16 (2004) 2102.
[22] Y.C. Fang, Z.J. Zhang, Z.Q. Xie, Y.Y. Zhao, M. Lu, Appl. Phys. Lett. 86 (2005) 191919.
[23] M. Boufard, J.P. Jouart, M.F. Joubert, Opt. Mater. 14 (2000) 73.
[24] V. Grover, S.N. Achary, S.J. Patwe, A.K. Tyagi, Mater. Res. Bull. 38 (2003) 1413.
[25] R. Singh, S. Sinha, P. Chou, N.J. Hsu, F. Radpour, J. Appl. Phys. 66 (1989) 6179.
[26] A.J. Wojtowicz, Nucl. Instrum. Meth. A 486 (2002) 201.
[27] R.N. Grass, W.J. Stark, Chem. Commun. (2005) 1767.
[28] H.Z. Lian, J. Liu, Z.R. Ye, C.S. Shi, Chem. Phys. Lett. 386 (2004) 291.
[29] C.M. Bender, J.M. Burlitch, Chem. Mater. 12 (2000) 1969.
[30] G.J. De, W.P. Qin, J.S. Zhang, J.S. Zhang, Y. Wang, C.Y. Cao, Y. Cui, J. Solid State Chem. 179 (2006) 955.
[31] P. Gao, Y. Xie, Z. Li, Eur. J. Inorg. Chem. (2006) 3261.
[32] M.H. Cao, C.W. Hu, E.B. Wang, J. Am. Chem. Soc. 125 (2003) 11196.
[33] H.Z. Lian, Z.R. Ye, C.S. Shi, Nanotechnology 15 (2004) 1455.
[34] W.J. Crooks III, W.D. Rhodes, Use of Modeling for the Prevention of Solids Formation during Canyon Processing of Legacy Nuclear Materials, Westinghouse Savannah River Company Aiken, SC 29808, WSRC-TR-2002-00462, 2003, p. 7.
[35] B.R. Judd, Phys. Rev. 127 (1962) 750.
[36] G.S. Ofelt, J. Chem. Phys. 37 (1962) 511.
[37] X.C. Wu, Y.R. Tao, C.Y. Song, C.J. Mao, L. Dong, J.J. Zhu, J. Phys. Chem. B 110 (2006) 15791.
[38] L.M. Chen, Y.N. Liu, K.L. Huang, Mater. Res. Bull. 41 (2006) 158.
[39] Z.G. Wei, L.D. Sun, C.S. Liao, J.L. Yin, X.C. Jiang, C.H. Yan, J. Phys. Chem. B 106 (2002) 10610.